

Multiple Model \mathcal{L}_1 Adaptive Fault-Tolerant Control of Small Unmanned Aerial Vehicles

Toufik Souanef¹

¹Cranfield University, United Kingdom. Email: toufik.souanef@cranfield.ac.uk

ABSTRACT

This paper presents a method for fault-tolerant control of small fixed-wing Unmanned Aerial Vehicles (UAVs). The proposed design is based on multiple-model \mathcal{L}_1 adaptive control. The controller is composed of a nominal reference model and a set of suboptimal reference models. The nominal model is the one with desired dynamics that are optimal regarding some specific criteria. In a suboptimal model the performance criteria are reduced, it is designed to ensure system robustness in the presence of critical failures. The controller was tested in simulations and it was shown that the multiple model \mathcal{L}_1 adaptive controller stabilizes the system in case of inversion of the control input, while the \mathcal{L}_1 adaptive controller with a single nominal model fails.

INTRODUCTION

Unmanned Aerial Vehicles (UAVs), commonly known as drones and referred to as Remotely Piloted Aircraft (RPA) by the International Civil Aviation Organisation (ICAO), are aircraft without a human pilot aboard. According to the assigned missions or to their size, there are many different classes of UAVs (Valavanis and Vachtsevanos, 2015). This work focuses on small fixed-wing UAVs that is, with wingspans less than 2 metres and payload smaller than 2 kg. Small UAVs are gaining growing interest because of their low cost, high manoeuvrability, and simple maintenance. They are used for a wide range of military and civilian tasks (Austin, 2011). The operation of UAVs, especially in urban environments, needs a high degree of safety and reliability. However, small UAVs are generally built with low-cost components and materials, which increases the probability

24 of occurrence of faults and failures. For that reason, the design of fault-tolerant control systems is
25 required (Blanke et al., 2006; Ducard, 2009; Patton, 1997; Zhang and Jiang, 2008).

26 Fault-tolerant control is defined as a system that possesses the ability to accommodate failures
27 automatically (Zhang and Jiang, 2008). Fault-tolerant control systems are classified as either
28 passive or active (Hwang et al., 2009; Rotondo, 2017). Passive fault-tolerant control is based on
29 robust control while assuming the worst case conditions (Amin and Hasan, 2019; Benosman, 2011;
30 Edwards et al., 2000; Wang, 2010; Yang et al., 2001). Nevertheless, the designed controllers tend to
31 be conservative from performance viewpoint (Jiang and Yu, 2012). Active fault-tolerant controllers
32 are composed of a fault detection scheme and a supervision module. On the basis of the information
33 of the former, the supervision module may decide how to reconfigure the controller (Abbaspour
34 et al., 2020; Amin and Hasan, 2019; Rotondo, 2017). However, applying such advanced control
35 systems for small UAVs is difficult, because of their limited computing resources.

36 A compromise between the two approaches is adaptive control, which is based on the reconfig-
37 uration of the controller parameters without involving an explicit fault detection module (Bodson,
38 2003; Ma et al., 2020; Nian et al., 2020; Tao, 2004; Xue et al., 2020; Yang et al., 2014).

39 A crucial aspect in applying adaptive control techniques to real-world systems is the transient
40 response guarantee, in the absence of which, overly poor tracking behaviour can occur before
41 ideal asymptotic convergence takes place (Zang and Bitmead, 1990). Moreover, the transient
42 performance improvement cannot be achieved through high-gain feedback, which will degrade
43 the robustness of the closed-loop system. However, most adaptive control methods focus on the
44 asymptotic performance, providing no transient performance guarantee without resorting to high-
45 gain feedback. One solution to this issue is based on \mathcal{L}_1 adaptive control (Hovakimyan and Cao,
46 2010). The adaptive control architecture decouples the estimation loop from the control loop
47 through the introduction of a low-pass filter. As a result, arbitrarily fast adaptation can be used
48 without sacrificing system robustness. The benefit of \mathcal{L}_1 adaptive control is its capacity for fast and
49 robust adaptation that leads to desired transient performance for both system signals, inputs and
50 outputs. These characteristics make it suitable for systems with unknown dynamics and subject to

51 possible faults and external disturbances, such as small UAVs.

52 Despite the excellent performance of \mathcal{L}_1 adaptive control, for fault-tolerant control (Ackerman
53 et al., 2017; Ahmadi et al., 2019; Dobrokhodov et al., 2013; Mühlegg et al., 2015; Patel et al.,
54 2009; Sørensen and Breivik, 2015; Tian et al., 2020; Zhou et al., 2019), it is still true that when
55 the uncertainties induced by disturbances, faults or failures are too large, they may reduce the
56 performance of the controller or even make the system unstable. Actually, if a fault or a failure occurs
57 on the system, the unknown parameters may go outside the predefined sets of the control design,
58 which may lead to poor system performance or more critically to system instability. Furthermore,
59 when a fault affects the system actuators it reduces their capabilities and, if the nominal performance
60 of the system is maintained, the actuators will work beyond their nominal set point, which might
61 lead to severe failures that cannot be compensated by a fault-tolerant controller. Therefore, it is not
62 reasonable to maintain the same desired performance of the system, because after a fault or a failure
63 it is not possible to recover the nominal performance. This is especially true for non-redundant
64 systems such as low-cost UAVs.

65 The proposed solution is based on the application of the multiple model \mathcal{L}_1 adaptive controller
66 (Souanef and Fichter, 2015). The key idea is to design an \mathcal{L}_1 adaptive controller with a nominal
67 reference model and a set of suboptimal reference models. The nominal model is the model with
68 desired dynamics that are optimal regarding some specific criteria. A suboptimal model does not
69 necessarily verify these specifications. It is designed to ensure system robustness in the presence of
70 large uncertainties. This multiple-model \mathcal{L}_1 adaptive control design can expand the performance
71 of the \mathcal{L}_1 adaptive control schemes to effectively deal with plant hard failures such as the inversion
72 of the control direction (a long-standing issue that is difficult for a single-model adaptive controller
73 to deal with) which may be caused by uncertain system structural damage and component (actuator
74 or sensor) failures.

75 A similar approach for performance degradation based on multiple model control was presented
76 in (Jiang and Zhang, 2006; Zhang and Jiang, 2003). The design was made under the assumption that
77 the model of the plant has no uncertainties, which is not realistic, especially for post-fault systems.

78 Furthermore, only actuator faults were addressed while structural faults were not considered.

79 The main contributions of this paper are:

- 80 • Development of a method for adaptive fault-tolerant control based on an \mathcal{L}_1 adaptive
81 controller with a nominal reference model and a set of suboptimal reference models, so as
82 to avoid system instability in the presence of hard faults/failures.
- 83 • Extension of the method proposed in (Souanef and Fichter, 2015) to Multi-Input Multi-
84 Output (MIMO) systems.

85 NOTATION

86 Throughout the paper, $\|\cdot\|$ denotes the 2-norm and $\|\cdot\|_\infty$ denotes the infinity norm of a vector or
87 a matrix. The notation $\|\xi\|_{\mathcal{L}_\infty}$ denotes the \mathcal{L}_∞ -norm of the vector $\xi(t)$. For a stable proper transfer
88 matrix $G(s)$, $\|G(s)\|_{\mathcal{L}_1}$ denotes its \mathcal{L}_1 -norm. \mathbb{R}^n denotes the n-dimensional real vector space.
89 \mathbb{I} denotes an identity matrix of appropriate dimensions. Boldface notation is used for matrices,
90 vectors, and tensors; italics are for for all variables and lower-case Greek letters; and Roman for all
91 numerals, upper-case Greek characters, and mathematical operators.

92 PROBLEM FORMULATION

93 For control design, the dynamic model of an aircraft can be formulated as the following class
94 of MIMO systems (Lavretsky and Wise, 2013)

$$\begin{aligned} \dot{\mathbf{x}}(t) &= \mathbf{A}_p \mathbf{x}(t) + \mathbf{B}_p \mathbf{u}_p(t) + \mathbf{f}(t, \mathbf{x}), \quad \mathbf{x}(0) = \mathbf{x}_0, \\ \mathbf{y}(t) &= \mathbf{C} \mathbf{x}(t), \end{aligned} \tag{1}$$

96 where $\mathbf{A}_p = \mathbf{A} + \Delta \mathbf{A} \in \mathbb{R}^{n \times n}$ is an unknown matrix, $\mathbf{A} \in \mathbb{R}^{n \times n}$ is a known matrix, $\Delta \mathbf{A} \in \mathbb{R}^{n \times n}$
97 an unknown matrix of the system dynamics, $\mathbf{B}_p = \mathbf{B}(\mathbb{I}_m + \Delta \mathbf{B}) \in \mathbb{R}^{n \times m}$ is an unknown matrix,
98 $\mathbf{B} \in \mathbb{R}^{n \times m}$ is a known matrix, $\Delta \mathbf{B} \in \mathbb{R}^{m \times m}$ is an unknown matrix of the control input uncertainties,
99 $\mathbf{C} \in \mathbb{R}^{m \times n}$ is a known matrix, $\mathbf{x}(t) \in \mathbb{R}^n$ is the state vector which is assumed to be available through
100 measurement, $\mathbf{u}_p(t) \in \mathbb{R}^m$ is the control input vector $\mathbf{y}(t) \in \mathbb{R}^m$ is the output vector and $\mathbf{f}(t, \mathbf{x}) \in \mathbb{R}^n$
101 is a vector of unknown nonlinear functions.

102 Now consider the control

$$103 \quad \mathbf{u}_p(t) = \mathbf{u}(t) + \mathbf{K}_l \mathbf{x}(t), \quad (2)$$

104 where $\mathbf{K}_l \in \mathbb{R}^{m \times n}$ is a gain matrix that defines $\mathbf{A}_m = \mathbf{A} + \mathbf{B}\mathbf{K}_l$, where $\mathbf{A}_m \in \mathbb{R}$ is a Hurwitz matrix
 105 that defines the desired dynamics of the system. The resulting system to be controlled by the
 106 adaptive control is

$$107 \quad \dot{\mathbf{x}}(t) = \mathbf{A}_m \mathbf{x}(t) + \mathbf{B}\omega \mathbf{u}(t) + \tilde{\mathbf{f}}(t, \mathbf{x}), \quad (3)$$

108 where $\omega = \mathbb{I}_m + \Delta \mathbf{B}$ and $\tilde{\mathbf{f}}(t, \mathbf{x}) = \Delta \mathbf{A} \mathbf{x}(t) + (\omega - \mathbb{I}_m) \mathbf{K}_l \mathbf{x}(t) + \mathbf{f}(t, \mathbf{x})$. Assuming $\tilde{\mathbf{f}}(t, \mathbf{x}) = \mathbf{B}(\theta^\top \mathbf{x}(t) +$
 109 $\eta_m(t)) + \eta_u(t)$, the system in (3) can be parametrised as follows

$$110 \quad \dot{\mathbf{x}}(t) = \mathbf{A}_m \mathbf{x}(t) + \mathbf{B}(\omega \mathbf{u}(t) + \theta^\top \mathbf{x}(t) + \eta_m(t)) + \eta_u(t), \quad (4)$$

111 where $\theta^\top \in \mathbb{R}^{m \times n}$ is a matrix of constant unknown parameters representing model uncertainties,
 112 $\eta_m(t) \in \mathbb{R}^m$ is an unknown matched disturbance, and $\eta_u(t) \in \mathbb{R}^n$ is an unknown unmatched
 113 disturbance.

114 **Assumption 1.** The unknown model parameters are bounded, i.e., $\theta \in \Theta$, where Θ is a known
 115 compact convex set. The system input gain matrix ω is assumed to be an unknown (non-singular)
 116 strictly row-diagonally dominant matrix with $\text{sgn}(\omega_{ii})$ known. Also, it is assumed that there exists
 117 a known compact convex set Ω such that $\omega \in \Omega \subset \mathbb{R}^{m \times m}$.

Assumption 2. The non-linear function $\eta_m(t)$ is uniformly bounded, i.e., there exist unknown
 real constant $L_m > 0$, such that for all $t \geq 0$ the following bound hold:

$$\|\eta_m(t)\| \leq L_m.$$

Assumption 3. There exist unknown real constant $L_u > 0$, such that for all $t \geq 0$ the following

bound hold

$$\|\eta_u(t)\| \leq L_u.$$

118 **Remark 1.** Assumptions 2 and 3 are acceptable for real systems, given that a superior bound
 119 of disturbances, which the system may hold without being broken, is usually known from technical
 120 specifications or engineering insights.

121 The objective is to design a state-feedback controller to ensure that the output of the system
 122 tracks a given piecewise continuous bounded reference signal $r(t)$ and consequently maintain the
 123 stability of the control system despite the presence of faults and/or external disturbances.

124 \mathcal{L}_1 ADAPTIVE CONTROL

125 We consider the architecture of the \mathcal{L}_1 adaptive controller which is composed of the state
 126 predictor, the adaptation law and the control law (Figure 1).

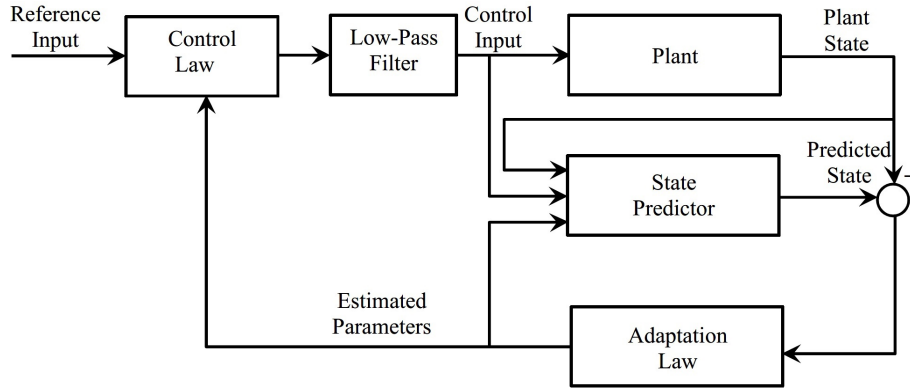


Fig. 1. Block diagram of the \mathcal{L}_1 adaptive controller.

127 The state predictor is defined as

$$128 \quad \hat{\mathbf{x}}(t) = \mathbf{A}_m \hat{\mathbf{x}}(t) + \mathbf{B}(\hat{\omega}(t)\mathbf{u}(t) + \hat{\theta}^\top(t)\mathbf{x}(t) + \hat{\eta}_m(t)) + \hat{\eta}_u(t), \quad (5)$$

129 where $\hat{\mathbf{x}}(t)$ is the predicted state and $\hat{\theta}(t)$, $\hat{\omega}(t)$, $\hat{\eta}_m(t)$, and $\hat{\eta}_u(t)$ are the estimates of the unknown
 130 system parameters and disturbances.

131 The sliding surface is defined as

$$132 \quad \sigma(t) = \lambda \tilde{\mathbf{x}}(t), \quad (6)$$

133 where $\tilde{\mathbf{x}}(t) = \hat{\mathbf{x}}(t) - \mathbf{x}(t)$ is the state estimation error and $\lambda \in \mathbb{R}^{m \times n}$ is a constant arbitrary matrix,
 134 chosen such that $\lambda \mathbf{B}$ is non-singular and the coefficients $\lambda(i, j) : i = 1..n; j = 1..m$ form a stable
 135 hyperplane.

136 The estimation of the matched disturbance $\eta_m(t)$ is defined by

$$137 \quad \hat{\eta}_m(t) = \begin{cases} -(\lambda \mathbf{B})^{-1} (\lambda \mathbf{A}_m \tilde{\mathbf{x}}(t) + \rho \sigma(t)) - \hat{L}_m(t) \frac{\mathbf{B}^\top \lambda^\top \sigma(t)}{\|\mathbf{B}^\top \lambda^\top \sigma(t)\|}, & \text{if } \sigma(t) \neq 0, \\ 0 & \text{otherwise,} \end{cases} \quad (7)$$

138 where $\rho > 0$ is arbitrary and the estimated bound $\hat{L}_m(t)$ is given by

$$139 \quad \hat{L}_m(t) = \Gamma \|\sigma^\top(t) \lambda \mathbf{B}\|, \quad (8)$$

140 where $\Gamma \in \mathbb{R}^+$ is the adaptation rate.

141 The estimation of the unmatched disturbance $\eta_u(t)$ is defined by

$$142 \quad \hat{\eta}_u(t) = \begin{cases} -\hat{L}_u(t) \frac{\lambda^\top \sigma(t)}{\|\lambda^\top \sigma(t)\|}, & \text{if } \sigma(t) \neq 0, \\ 0 & \text{otherwise,} \end{cases} \quad (9)$$

143 where the estimated bound $\hat{L}_u(t)$ is computed by

$$144 \quad \hat{L}_u(t) = \Gamma \|\sigma^\top(t) \lambda\|, \quad (10)$$

145 The input gain matrix ω and unknown parameters matrix θ are estimated by

$$\begin{aligned}
 \dot{\hat{\omega}}(t) &= -\Gamma \text{Proj}(\hat{\omega}(t), \mathbf{u}(t) \sigma^\top(t) \lambda \mathbf{B})^\top, \\
 \dot{\hat{\theta}}(t) &= -\Gamma \text{Proj}(\hat{\theta}(t), \mathbf{x}(t) \sigma^\top(t) \lambda \mathbf{B}).
 \end{aligned}
 \tag{11}$$

147 The control law is given by

$$\mathbf{u}(s) = -\mathbf{K} \mathbf{D}(s) \left(\hat{v}_1(s) + \hat{v}_2(s) - \mathbf{K}_g \mathbf{r}(s) \right),
 \tag{12}$$

149 where $\mathbf{D}(s)$ is an $m \times m$ proper transfer matrix; $\mathbf{K} \in \mathbb{R}^{m \times m}$; $\mathbf{K}_g = -(\mathbf{C} \mathbf{A}_m^{-1} \mathbf{B})^{-1}$ is the pre-filter
 150 of the MIMO control law; $\hat{v}_1(s)$ is the Laplace transformation of $\hat{v}_1(t) = \hat{\theta}^\top(t) \mathbf{x}(t) + \hat{\omega}(t) \mathbf{u}(t)$;
 151 $\mathbf{H}_m(s) = \mathbf{C}(s\mathbb{I} - \mathbf{A}_m)^{-1} \mathbf{B}$; $\mathbf{H}_0(s) = \mathbf{C}(s\mathbb{I} - \mathbf{A}_m)^{-1}$; and $\hat{v}_2 = \hat{\eta}_m(t) + \mathbf{H}_m^{-1}(s) \mathbf{H}_0(s) \hat{\eta}_u(s)$.

The design of $\mathbf{D}(s)$ and \mathbf{K} should lead to a strictly proper and stable filter transfer matrix

$$\mathbf{F}(s) = \omega \mathbf{K} \mathbf{D}(s) (\mathbb{I} + \omega \mathbf{K} \mathbf{D}(s))^{-1},$$

152 with static gain $\mathbf{F}(0) = \mathbb{I}$.

153 Let

$$\begin{aligned}
 L &= \max_{\theta \in \Theta} \|\theta\|_1, \quad \mathbf{H}(s) = (s\mathbb{I} - \mathbf{A}_m)^{-1} \mathbf{B}, \\
 \mathbf{G}(s) &= \mathbf{H}(s) (\mathbb{I} - \mathbf{F}(s)).
 \end{aligned}
 \tag{13}$$

155 The \mathcal{L}_1 adaptive controller is subject to the \mathcal{L}_1 norm condition

$$\|\mathbf{G}(s)\|_{\mathcal{L}_1} L < 1.
 \tag{14}$$

157 Moreover, the design of $\mathbf{F}(s)$ needs to ensure that

$$\mathbf{G}_u(s) = (s\mathbb{I} - \mathbf{A}_m)^{-1} - \mathbf{F}(s) \mathbf{H}(s) \mathbf{H}_m^{-1}(s) \mathbf{H}_0(s),
 \tag{15}$$

159 is proper and stable. Furthermore, since the transfer matrix $\mathbf{G}_u(s)$ is proper and stable it has an \mathcal{L}_1
 160 norm (Hovakimyan and Cao, 2010).

161 **Remark 2.** It has been shown in (Souanef et al., 2015) and (Souanef, 2019) that the adaptation
 162 laws of the external disturbances in equations (7) and (9) use the estimated bounds from equations (8)
 163 and (10). This relaxes the assumption that the bounds of the external disturbances are known, which
 164 is required in \mathcal{L}_1 adaptive control based on projection-type adaptive laws (Cao and Hovakimyan,
 165 2008).

166 **Remark 3.** If a fault or failure occurs on the system, the unknown parameters may go outside
 167 the predefined sets. Therefore, the stability conditions in (14) and (15) may become not satisfied.
 168 Hence, it is necessary to maintain system stability and a minimum of good performance, this is done
 169 through the design of a set of suboptimal models which become effective when large uncertainties
 170 appear on the plant.

171 MULTIPLE MODEL \mathcal{L}_1 ADAPTIVE CONTROL OF MIMO SYSTEMS

172 Considering probable faults scenario, a set of plant parameterisations, based on multiple models,
 173 is arranged, and the objective is that the satisfactory controller is selected automatically to deal
 174 with every situation. This means that the model which is the best match of the plant is selected.

175 The desired performance of each model is made through the design of the pair $(\mathbf{A}_{m(i)}, \mathbf{B}_i)$, for
 176 $i \in \mathcal{I}$.

177 The system in (1) can consequently be parameterised as follows

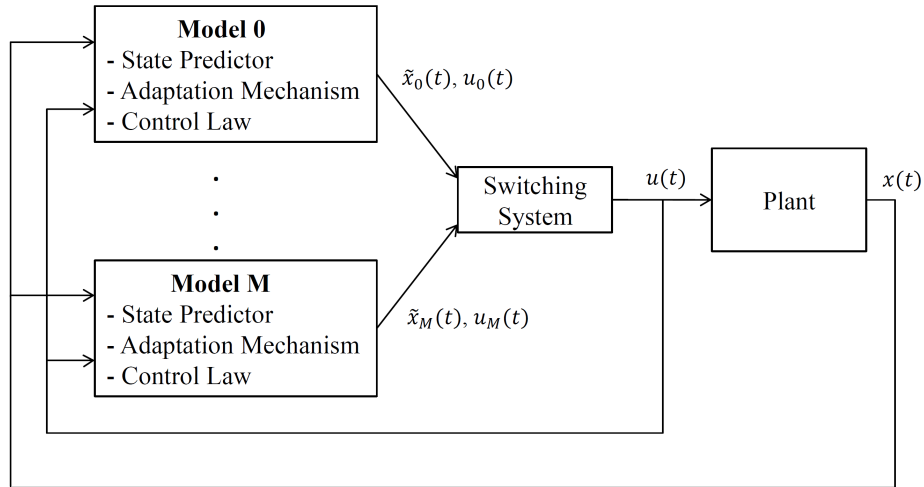
$$178 \quad \dot{\mathbf{x}}(t) = \mathbf{A}_{m(i)}\mathbf{x}(t) + \mathbf{B}_i(\omega_i\mathbf{u}(t) + \theta_i^\top\mathbf{x}(t) + \eta_{m(i)}(t)) + \eta_{u(i)}(t), \quad (16)$$

179 where $\mathbf{A}_{m(i)} \in \mathbb{R}^{n \times n}$ are known Hurwitz matrices that define the desired dynamics of the system
 180 $\mathbf{B}_i \in \mathbb{R}^{n \times m}$ are the desired input matrices, $\omega_i \in \mathbb{R}^{m \times m}$ are unknown constant matrices representing
 181 the system input gain, $\theta_i^\top \in \mathbb{R}^{m \times n}$ are matrices of constant unknown parameters representing model
 182 uncertainties, $\eta_{m(i)}(t) \in \mathbb{R}^m$ are unknown matched disturbances, and $\eta_{u(i)}(t) \in \mathbb{R}^n$ are unknown
 183 unmatched disturbances.

184 **Assumption 4.** The system input gain matrices ω_i are assumed to be unknown (non-singular)
 185 strictly row-diagonally dominant matrices with known signs of diagonals. Also, it is assumed that
 186 the unknown parameters are bounded, i.e., $\theta_i \in \Theta_i$, where Θ_i are known compact convex sets.
 187 Furthermore, the functions $\eta_{m(i)}$ and $\eta_{u(i)}$ are uniformly bounded, i.e., there exist unknown real
 188 constants $L_{m(i)} > 0$ and $L_{u(i)} > 0$, such that for all $t \geq 0$ $|\eta_{m(i)}(t)| \leq L_{m(i)}$ and $\|\eta_{u(i)}(t)\| \leq L_{u(i)}$.

189 Controller Design

190 The multiple model \mathcal{L}_1 adaptive controller, as shown in Figure 2, is composed of a set of state
 191 predictors, a set of adaptation laws, a set of control laws and a control input selector (switching
 system). The state predictors are defined by



192 **Fig. 2.** Block diagram of the multiple model \mathcal{L}_1 adaptive controller.

$$193 \quad \dot{\hat{\mathbf{x}}}_i(t) = \mathbf{A}_{m(i)} \hat{\mathbf{x}}_i(t) + \mathbf{B}_i (\hat{\omega}_i(t) \mathbf{u}(t) + \hat{\theta}_i^\top(t) \mathbf{x}(t) + \hat{\eta}_{m(i)}(t)) + \hat{\eta}_{u(i)}(t), \quad (17)$$

194 where $\hat{\mathbf{x}}_i(t)$ are the predicted states and, $\hat{\theta}_i(t)$, $\hat{\omega}_i(t)$, $\hat{\eta}_{m(i)}(t)$, and $\hat{\eta}_{u(i)}(t)$ are the estimates of the
 195 unknown system parameters and external disturbances. The initial state of the state predictor is
 196 equal to the plant state at switching time t_k :

$$197 \quad \hat{\mathbf{x}}(t_k) = \mathbf{x}(t_k). \quad (18)$$

198 The sliding surfaces are given by

$$199 \quad \sigma_i(t) = \lambda_i \tilde{\mathbf{x}}_i(t), \quad (19)$$

200 where $\tilde{\mathbf{x}}_i(t) = \hat{\mathbf{x}}_i(t) - \mathbf{x}(t)$ are the state estimation errors and $\lambda_i \in \mathbb{R}^{m \times n}$ are constant arbitrary
 201 matrices, chosen such that $\lambda_i \mathbf{B}_i$ are non-singular and the coefficients $\lambda_i(k, j) : k = 1 \dots n; j = 1 \dots m$
 202 form a stable hyperplane.

203 The adaptation laws are given by

$$204 \quad \begin{aligned} \dot{\hat{\omega}}_i(t) &= -\Gamma_i \text{Proj}(\mathbf{u}(t) \sigma_i^\top \lambda_i \mathbf{B}_i)^\top, \\ \dot{\hat{\theta}}_i(t) &= -\Gamma_i \text{Proj}(\mathbf{x}(t) \sigma_i^\top \lambda_i \mathbf{B}_i), \\ \hat{\eta}_{m(i)}(t) &= \begin{cases} -(\lambda_i \mathbf{B}_i)^{-1} (\lambda_i \mathbf{A}_{m(i)} \tilde{\mathbf{x}}_i(t) + \rho_i \sigma_i) - \hat{L}_{m(i)}(t) \frac{\mathbf{B}_i^\top \lambda_i^\top \sigma_i}{\|\mathbf{B}_i^\top \lambda_i^\top \sigma_i\|} & \text{if } \sigma_i \neq 0, \\ 0 & \text{if not,} \end{cases} \\ \hat{\eta}_{u(i)}(t) &= \begin{cases} -\hat{L}_{u(i)}(t) \frac{\lambda_i^\top \sigma_i}{\|\lambda_i^\top \sigma_i\|} & \text{if } \sigma_i \neq 0, \\ 0 & \text{if not,} \end{cases} \\ \dot{\hat{L}}_{m(i)}(t) &= \Gamma_i \|\sigma_i^\top \lambda_i \mathbf{B}_i\|, \\ \dot{\hat{L}}_{u(i)}(t) &= \Gamma_i \|\sigma_i^\top \lambda_i\|, \end{aligned} \quad (20)$$

205 where $\rho_i > 0$ are arbitrary and $\Gamma_i \in \mathbb{R}^+$ are the adaptation rates.

Let

$$\mathbf{H}_{m(i)}(s) = \mathbf{C}_i (s\mathbb{I} - \mathbf{A}_{m(i)})^{-1} \mathbf{B}_i \text{ and } \mathbf{H}_{0(i)}(s) = \mathbf{C}_i (s\mathbb{I} - \mathbf{A}_{m(i)})^{-1}.$$

206 The control laws are given by

$$207 \quad \mathbf{u}_i(s) = -\mathbf{K}_i \mathbf{D}_i(s) \left(\mathbf{K}_{g(i)} \mathbf{r}(s) - \hat{v}_{(i)}(s) \right), \quad (21)$$

208 where $\hat{v}_{(i)}(s) = \hat{v}_{1(i)}(s) + \hat{v}_{2(i)}(s)\hat{\eta}_{u(i)}(s)$, $\hat{v}_{1(i)}(s)$ are the Laplace transformations of $\hat{v}_{1(i)}(t) =$
 209 $\hat{\theta}_i^\top(t)\mathbf{x}(t) + \hat{\omega}_i(t)\mathbf{u}_i(t)$, $\hat{v}_{2(i)}(s) = \hat{\eta}_{m(i)}(s) + \mathbf{H}_{m(i)}^{-1}(s)\mathbf{H}_{0(i)}(s)\hat{\eta}_{u(i)}(s)$, $\mathbf{K}_{g(i)} = -(\mathbf{C}_i\mathbf{A}_{m(i)}^{-1}\mathbf{B}_i)^{-1}$ are
 210 the pre-filters of the MIMO control laws, $\mathbf{D}_i(s)$ are $m \times m$ strictly proper transfer matrices and
 211 $\mathbf{K}_i \in \mathbb{R}^{m \times m}$.

212 Let $\mathbf{B}_i^\dagger = (\mathbf{B}_i^\top \mathbf{B}_i)^{-1} \mathbf{B}_i^\top$ be the pseudo-inverse of \mathbf{B}_i , considering that \mathbf{B}_i has full column rank,
 213 then $\hat{v}_{2(i)}(t) = \hat{\eta}_{m(i)}(t) + \mathbf{B}_i^\dagger \hat{\eta}_{u(i)}(t)$.

214 For analysis purposes, without loss of generality, it is assumed that the control laws use the
 215 same filter parameters. $\mathbf{D}_i(s)$ are chosen $\mathbf{D}_i(s) = \frac{\mathbf{D}_0(s)}{s}$ and $\mathbf{K}_i = 1$, where $\mathbf{D}_0(s)$ is a proper stable
 216 transfer matrix.

217 Therefore, the control laws can be written as

$$218 \quad \mathbf{u}_i(s) = \frac{\mathbf{D}_0(s)}{s} \left(\mathbf{K}_{g(i)} \mathbf{r}(s) - \hat{v}_{(i)}(s) \right). \quad (22)$$

219 The switching logic is defined by

$$220 \quad \min_{i \in \mathcal{I}} \left\{ J_i = c_1 \|\tilde{\mathbf{x}}_i\|^2 + c_2 \int_0^t e^{-c_3(t-\tau)} \|\tilde{\mathbf{x}}_i(\tau)\|^2 d\tau \right\}, \quad (23)$$

221 where c_1, c_2 and c_3 are arbitrary positive real. The model that minimises the criterion becomes the
 222 selected model and its output is applied to the plant.

223 **Remark 4.** For practical implementation the discrete-time version of the switching logic in
 224 (23) is given by

$$225 \quad \min_{i \in \mathcal{I}} \left\{ J_i = c_1 \|\tilde{\mathbf{x}}_i(kT)\|^2 + \frac{c_2}{c_3 kT + 1} \sum_{j=0}^j \|\tilde{\mathbf{x}}_i(jT)\|^2 \right\}, \quad (24)$$

226 where T is the sampling period.

227 **Remark 5.** It is assumed in this work that the switching is arbitrary, i.e., not dwell time or average
 228 dwell time. To prevent arbitrarily fast switching, a non-zero waiting time $T_{min} > 0$ is introduced after
 229 every switching. By the end of the waiting period T_{min} , the controller corresponding to the model
 230 with the minimum index is chosen (switched) to control the plant Narendra and Balakrishnan

231 (1997). Note that T_{min} is different from the dwell time τ , and a switching signal has a dwell
232 time $\tau > 0$, used for waiting another controller being activated, if the switching times satisfy
233 $t_{k+1} - t_k \geq \tau, \forall k > 0$ (Liberzon, 2003).

234 **Remark 6.** It is a common practice to stop the control switching when $J_i(t) \leq \epsilon \forall i = 1, 2, \dots, N$,
235 for some pre-chosen, arbitrary and small $\epsilon > 0$ Tan et al. (2017a).

236 **Remark 7.** It is quiet understood that both traditional projection-based adaptive law (Cao and
237 Hovakimyan, 2008) and the piecewise-constant adaptive law (Cao and Hovakimyan, 2009) can be
238 applied to the design of the multiple model \mathcal{L}_1 adaptive controller. The advantage of the sliding
239 mode adaptation law is that it permits to estimate the upper bounds of the external disturbances
240 which makes the system more robust.

241 **Controller Analysis**

242 In this section, the performance of the \mathcal{L}_1 adaptive controller is analysed. More specifically it
243 is shown that:

- 244 • The reference models resulting from perfect knowledge of the uncertainties and a corre-
245 sponding non-adaptive controller are stable, subject to some conditions involving the filter
246 $D_0(s)$.
- 247 • The prediction errors, i.e. the errors between the states of the plant and those of the state
248 predictors, are bounded.
- 249 • The differences between the states/input of the system and those of the reference systems
250 are proportional to the prediction error

251 For a switching system, it is not straightforward to compute the \mathcal{L}_1 norm condition in (14) and
252 (15). Actually, for Linear Time Invariant (LTI) systems, the \mathcal{L}_1 norm is readily computed from
253 the impulse response. However, for a switched system, the impulse response is time dependent
254 (switching signal-dependent), and computing the \mathcal{L}_1 norm is not as straightforward as in the LTI
255 case.

256 A similar approach to (Snyder, 2019) is applied here. It is based on a new method of analysing

257 \mathcal{L}_1 adaptive control. This approach results in necessary and sufficient conditions provided in the
 258 form of linear matrix inequalities (LMIs).

259 *Reference Models Analysis*

260 The reference system with the nominal parameters is defined as follows

$$261 \begin{aligned} \dot{\mathbf{x}}_r(t) &= \mathbf{A}_{m(i)} \mathbf{x}_r(t) + \mathbf{B}_i (\omega_i \mathbf{u}_r(t) + \theta_i^\top \mathbf{x}_r(t) + \eta_{m(i)}(t)) + \eta_{u(i)}(t), \quad \mathbf{x}_r(0) = \mathbf{x}_0 \\ \mathbf{u}_r(s) &= - \frac{\mathbf{D}_0(s)}{s} (\nu_{r(i)}(s) - \mathbf{K}_g(i) \mathbf{r}(s)) \end{aligned} \quad (25)$$

262 where $\nu_{r(i)}(s) = \nu_{1(i)}(s) + \nu_{2(i)}(s)$, $\nu_{1(i)}(s)$ are the Laplace transformations of $\nu_{1(i)}(t) = \theta_i^\top \mathbf{x}_r(t) + \omega_i(t) \mathbf{u}_r(t)$
 263 and $\nu_{2(i)}(s) = \eta_{m(i)}(s) + \phi_i(s) \eta_{u(i)}(s)$, with $\phi_i(s) = \mathbf{H}_{m(i)}^{-1}(s) \mathbf{H}_{0(i)}(s)$.

264 Alternatively we can write $\nu_{2(i)}(t) = \eta_{m(i)}(t) + \mathbf{B}_i^\dagger \eta_{u(i)}(t)$.

265 **Remark 8.** It should be noted that the reference control law is not implementable, since it
 266 depends on the unknown parameters and it is used only for analysis purposes.

267 Letting $(\mathbf{A}_f, \mathbf{B}_f, \mathbf{C}_f, \mathbf{D}_f)$ be a minimal realisation of $\mathbf{D}_0(s)$ with n_f states, the reference system
 268 dynamics can be written in state-space form

$$269 \begin{aligned} \begin{bmatrix} \dot{\mathbf{x}}_r(t) \\ \dot{\mathbf{x}}_{f_1}(t) \\ \dot{\mathbf{x}}_{I_1}(t) \end{bmatrix} &= \underbrace{\begin{bmatrix} \mathbf{A}_{m(i)} + \mathbf{B}_i \theta_i^\top & 0 & -\mathbf{B}_i \omega_i \\ \mathbf{B}_f \theta_i^\top & \mathbf{A}_f & \mathbf{B}_f \omega_i \\ \mathbf{D}_f \theta_i^\top & \mathbf{C}_f & \mathbf{D}_f \omega_i \end{bmatrix}}_{\bar{\mathbf{A}}_i} \begin{bmatrix} \mathbf{x}_r(t) \\ \mathbf{x}_{f_1}(t) \\ \mathbf{x}_{I_1}(t) \end{bmatrix} \\ &+ \underbrace{\begin{bmatrix} \mathbf{B}_i \\ \mathbf{B}_f \\ \mathbf{D}_f \end{bmatrix}}_{\bar{\mathbf{B}}_i} \nu_{2(i)}(t) - \begin{bmatrix} 0 \\ \mathbf{B}_f \mathbf{K}_g i \\ \mathbf{D}_f \mathbf{K}_g i \end{bmatrix} r(t) \end{aligned} \quad (26)$$

$$\begin{aligned} [u_r(t)] &= \underbrace{\begin{bmatrix} 0 & 0 & -\mathbb{I} \end{bmatrix}}_{\bar{\mathbf{C}}} \begin{bmatrix} \mathbf{x}_r(t) \\ \mathbf{x}_{f_1}(t) \\ \mathbf{x}_{I_1}(t) \end{bmatrix}, \quad \begin{bmatrix} \mathbf{x}_r(0) \\ \mathbf{x}_{f_1}(0) \\ \mathbf{x}_{I_1}(0) \end{bmatrix} = \begin{bmatrix} \mathbf{x}_0 \\ 0 \\ 0 \end{bmatrix}, \end{aligned}$$

270 where \mathbf{x}_{f_1} , \mathbf{x}_{I_1} are the states of $\mathbf{D}_0(s)$ and the integrator respectively.

271 The reference control law can be rewritten in more compact form as

$$\begin{aligned}
 \dot{\bar{\mathbf{x}}}(t) &= \bar{\mathbf{A}}_i \bar{\mathbf{x}}(t) + \bar{\mathbf{B}}_i v_{2(i)}(t) + \bar{\mathbf{E}}_i r(t), \quad \bar{\mathbf{x}}(0) = \bar{\mathbf{x}}_0, \\
 \mathbf{u}_r(t) &= \bar{\mathbf{C}} \bar{\mathbf{x}}(t),
 \end{aligned}
 \tag{27}$$

273 where $\bar{\mathbf{x}}^\top(t) \triangleq [\mathbf{x}_r^\top(t), \mathbf{x}_{f_1}^\top(t), \mathbf{x}_I^\top(t)]$.

Lemma 2 Give an arbitrary matrix $\mathbf{Q} = \mathbf{Q}^\top > 0$, if there exists a constant symmetric matrix $\mathbf{P} > 0$ verifying

$$\bar{\mathbf{A}}_i^\top \mathbf{P} + \mathbf{P} \bar{\mathbf{A}}_i \leq -\mathbf{Q}, \quad \forall \theta_i \in \Theta_i \text{ and } \forall \omega_i \in \Omega_i,$$

274 then the Lyapunov function $V = \bar{\mathbf{x}}^\top \bar{\mathbf{P}} \bar{\mathbf{x}}$ guarantees the stability of the switching reference systems
 275 in (27).

276 This fact is straightforward from the converse Lyapunov theorem for LTI systems.

277 *Transient Performance and Steady-State Performance*

278 In the following Lemma, it is stated that the prediction errors $\tilde{\mathbf{x}}_i(t)$ and the estimation errors of
 279 the unknown parameters are bounded.

280 **Lemma 3** The following bound holds for the norm of the prediction error $\forall i \in \mathcal{I}$

$$\|\tilde{\mathbf{x}}_i\|_{\mathcal{L}_\infty} \leq \delta,
 \tag{28}$$

282 where $\delta > 0$ is an arbitrary small real.

283 Furthermore, the prediction errors $\tilde{\mathbf{x}}_i(t)$ converge asymptotically to zero, i.e.,

$$\lim_{t \rightarrow \infty} \tilde{\mathbf{x}}_i(t) = 0.
 \tag{29}$$

285 **Proof.** The proof is omitted here because of lack of space. Interested readers are referred to

286 Souanef (2019).

Theorem. There exist positive constants κ_2 and κ_3 such that, for each model i the error between the actual system and the reference system is bounded by

$$\begin{aligned}\|\mathbf{x}_r(t) - \mathbf{x}(t)\| &\leq \kappa_2 \\ \|\mathbf{u}_r(t) - \mathbf{u}(t)\| &\leq \kappa_3.\end{aligned}$$

287 Furthermore, if the closed-loop system is stable then

$$288 \quad \lim_{t \rightarrow \infty} \|\mathbf{x}_r(t) - \mathbf{x}(t)\| = 0 \quad \text{and} \quad \lim_{t \rightarrow \infty} \|\mathbf{u}_r(t) - \mathbf{u}(t)\| \quad (30)$$

289 **Proof.** In this section, the dependence of the parameters on (t) is dropped unless it is not clear
290 from the context.

291 From (22) it can be written

$$292 \quad \mathbf{u}(s) = -\frac{D_0(s)}{s} \left(\omega_i \mathbf{u}(s) + v_i(s) + \tilde{v}_i(s) - \mathbf{K}g_i \mathbf{r}(s) \right), \quad (31)$$

293 where $\tilde{v}_{(i)}(s) = \tilde{v}_{1(i)}(s) + \tilde{v}_{2(i)}(s)$, $\tilde{v}_{1(i)}(s)$ are the Laplace transformations of $\tilde{v}_{1(i)} = \tilde{\theta}_i^\top \mathbf{x}(t) +$
294 $\tilde{\omega}_i(t) \mathbf{u}(t)$ and $\tilde{v}_{2(i)}(s) = \tilde{\eta}_{u(i)}(s) + \phi_i(s) \tilde{\eta}_{u(i)}(s)$.

295 Consequently, the closed-loop systems (16) and (31) can be written as follows

$$\begin{aligned}296 \quad \begin{bmatrix} \dot{\mathbf{x}} \\ \dot{\mathbf{x}}_{f_1} \\ \dot{\mathbf{x}}_{I_1} \end{bmatrix} &= \begin{bmatrix} \mathbf{A}_{m(i)} + \mathbf{B}_i \theta_i^\top & 0 & -\mathbf{B}_i \omega_i \\ \mathbf{B}_f \theta_i^\top & \mathbf{A}_f & \mathbf{B}_f \omega_i \\ \mathbf{D}_f \theta_i^\top & \mathbf{C}_f & \mathbf{D}_f \omega_i \end{bmatrix} \begin{bmatrix} \mathbf{x} \\ \mathbf{x}_{f_1} \\ \mathbf{x}_{I_1} \end{bmatrix} + \begin{bmatrix} \mathbf{B}_i \\ \mathbf{B}_f \\ \mathbf{D}_f \end{bmatrix} v_{2(i)} \\ &+ \begin{bmatrix} 0 \\ \mathbf{B}_f \\ \mathbf{D}_f \end{bmatrix} \tilde{v}_i - \begin{bmatrix} 0 \\ \mathbf{B}_f K g_i \\ \mathbf{D}_f K g_i \end{bmatrix} \mathbf{r}.\end{aligned} \quad (32)$$

297 The error between the state of the reference system and the actual plant, $e = x_r - x$, can be

298 expressed as

$$299 \begin{bmatrix} \dot{\mathbf{e}} \\ \dot{\mathbf{x}}_{f_1} \\ \dot{\mathbf{x}}_{I_1} \end{bmatrix} = \begin{bmatrix} \mathbf{A}_{m(i)} + \mathbf{B}_i \theta_i^\top & 0 & -\mathbf{B}_i \omega_i \\ \mathbf{B}_f \theta_i^\top & \mathbf{A}_f & \mathbf{B}_f \omega_i \\ \mathbf{D}_f \theta_i^\top & \mathbf{C}_f & \mathbf{D}_f \omega_i \end{bmatrix} \begin{bmatrix} e \\ x_{f_1} \\ x_{I_1} \end{bmatrix} + \begin{bmatrix} \mathbf{B}_i \\ \mathbf{B}_f \\ \mathbf{D}_f \end{bmatrix} \tilde{\mathbf{v}}_i. \quad (33)$$

300 The control error can also be formulated as follows

$$301 \mathbf{e}_u = \mathbf{u}_r - \mathbf{u} = \begin{bmatrix} 0 & 0 & -\mathbb{I} \end{bmatrix} \begin{bmatrix} \mathbf{e} \\ \mathbf{x}_{f_1} \\ \mathbf{x}_{I_1} \end{bmatrix}. \quad (34)$$

302 From (16) and (17), the prediction error dynamics can be written as

$$303 \dot{\tilde{\mathbf{x}}}_i = \mathbf{A}_{m(i)} \tilde{\mathbf{x}}_i + \mathbf{B}_i (\tilde{\omega}_i \mathbf{u} + \tilde{\theta}_i^\top \mathbf{x} + \tilde{\eta}_{m(i)}) + \tilde{\eta}_{u(i)}. \quad (35)$$

304 Thus

$$305 \tilde{\mathbf{v}}_i = \mathbf{B}_i^\dagger (\dot{\tilde{\mathbf{x}}}_i - \mathbf{A}_{m(i)} \tilde{\mathbf{x}}_i). \quad (36)$$

306 Passing $\mathbf{B}_i^\dagger \dot{\tilde{\mathbf{x}}}_i$ through the filter $(s\mathbb{I} + D_0(s)\omega_i)^{-1} D_0(s)$, we can write

$$307 \begin{bmatrix} \dot{\mathbf{x}}_{f_2} \\ \dot{\mathbf{x}}_{I_2} \end{bmatrix} = \begin{bmatrix} \mathbf{A}_f & \mathbf{B}_f \omega_i \\ \mathbf{C}_f & \mathbf{D}_f \omega_i \end{bmatrix} \begin{bmatrix} x_{f_2} \\ x_{I_2} \end{bmatrix} + \begin{bmatrix} \mathbf{B}_f \\ \mathbf{D}_f \end{bmatrix} \mathbf{B}_i^\dagger \dot{\tilde{\mathbf{x}}}_i. \quad (37)$$

Applying this to the error dynamics in (33) we have

$$\begin{aligned}
 \begin{bmatrix} \dot{\mathbf{e}} \\ \dot{\mathbf{x}}_{f_1} \\ \dot{\mathbf{x}}_{I_1} \\ \dot{\mathbf{x}}_{f_2} \\ \dot{\mathbf{x}}_{I_2} \end{bmatrix} &= \begin{bmatrix} \mathbf{A}_{m(i)} + \mathbf{B}_i \theta_i^\top & 0 & -\mathbf{B}_i \omega_i & -\mathbf{B}_i \mathbf{C}_f & -\mathbf{B}_i \mathbf{D}_f \omega_i \\ \mathbf{B}_f \theta_i^\top & \mathbf{A}_f & \mathbf{B}_f \omega_i & 0 & 0 \\ \mathbf{D}_f \theta_i^\top & \mathbf{C}_f & \mathbf{D}_f \omega_i & 0 & 0 \\ 0 & 0 & 0 & \mathbf{A}_f & \mathbf{B}_f \omega_i \\ 0 & 0 & 0 & \mathbf{C}_f & \mathbf{D}_f \omega_i \end{bmatrix} \begin{bmatrix} \mathbf{e} \\ \mathbf{x}_{f_1} \\ \mathbf{x}_{I_1} \\ \mathbf{x}_{f_2} \\ \mathbf{x}_{I_2} \end{bmatrix} \\
 &+ \begin{bmatrix} -\mathbf{D}_f \mathbf{B}_i^\dagger \\ -\mathbf{B}_f \mathbf{B}_i^\dagger \mathbf{A}_{m(i)} \\ -\mathbf{D}_f \mathbf{B}_i^\dagger \mathbf{A}_{m(i)} \\ -\mathbf{B}_f \mathbf{B}_i^\dagger \\ -\mathbf{D}_f \mathbf{B}_i^\dagger \end{bmatrix} \tilde{\mathbf{x}},
 \end{aligned} \tag{38}$$

and

$$\mathbf{e}_u = \begin{bmatrix} 0 & 0 & -\mathbb{I} & -\mathbf{C}_f & -\mathbf{D}_f \omega_i \end{bmatrix} \begin{bmatrix} \mathbf{e} \\ \mathbf{x}_{f_1} \\ \mathbf{x}_{I_1} \\ \mathbf{x}_{f_2} \\ \mathbf{x}_{I_2} \end{bmatrix} + \begin{bmatrix} -\mathbf{D}_f \mathbf{B}_i^\dagger \end{bmatrix} \tilde{\mathbf{x}}. \tag{39}$$

Letting

$$\begin{aligned}
 \bar{\mathbf{H}}_i &= \begin{bmatrix} -\mathbf{B}_i \mathbf{C}_f & -\mathbf{B}_i \mathbf{D}_f \omega_i \\ 0 & 0 \\ 0 & 0 \end{bmatrix}, \quad \bar{\mathbf{J}}_i = \begin{bmatrix} -\mathbf{D}_f \mathbf{B}_i^\dagger \\ -\mathbf{B}_f \mathbf{B}_i^\dagger \mathbf{A}_{m(i)} \\ -\mathbf{D}_f \mathbf{B}_i^\dagger \mathbf{A}_{m(i)} \end{bmatrix}, \\
 \bar{\mathbf{G}}_i &= \begin{bmatrix} -\mathbf{B}_f \mathbf{B}_i^\dagger \mathbf{A}_{m(i)} \\ -\mathbf{D}_f \mathbf{B}_i^\dagger \mathbf{A}_{m(i)} \end{bmatrix}, \quad \bar{\mathbf{L}}_i = \begin{bmatrix} 0 & \mathbf{C}_f & \mathbf{D}_f \omega_i \end{bmatrix},
 \end{aligned}$$

312 it follows from (38) and (39) that

$$313 \begin{bmatrix} \dot{\mathbf{e}} \\ \dot{\bar{\mathbf{x}}}_{f_2} \end{bmatrix} = \begin{bmatrix} \bar{\mathbf{A}}_i & \bar{\mathbf{H}}_i \\ 0 & \bar{\mathbf{F}}_i \end{bmatrix} \begin{bmatrix} \bar{\mathbf{e}} \\ \bar{\mathbf{x}}_{f_2} \end{bmatrix} + \begin{bmatrix} \bar{\mathbf{J}}_i \\ \bar{\mathbf{G}}_i \end{bmatrix} \tilde{\mathbf{x}}, \quad (40)$$

314 and

$$315 \mathbf{e}_u = \begin{bmatrix} \bar{\mathbf{C}} & \bar{\mathbf{L}}_i \end{bmatrix} \begin{bmatrix} \bar{\mathbf{e}} \\ \bar{\mathbf{x}}_{f_2} \end{bmatrix} + \begin{bmatrix} -\mathbf{D}_f \mathbf{B}_i^\dagger \end{bmatrix} \tilde{\mathbf{x}}, \quad (41)$$

316 where $\bar{\mathbf{e}} = [\mathbf{e}^\top, \mathbf{x}_{f_1}^\top, \mathbf{x}_{I_1}^\top]^\top$ and $\bar{\mathbf{x}}_{f_2} = [\mathbf{x}_{f_2}^\top, \mathbf{x}_{I_2}^\top]^\top$.

317 Note that the reference system is stable and the filter represented by $\bar{\mathbf{F}}_i$ is a subsystem of the
318 reference system when $\theta = 0$. Therefore, from Lemma 1, there exists positive definite matrices
319 $\mathbf{Q}_i(\omega_i) > 0$ such that for all $\omega_i \in \Omega$,

$$320 \bar{\mathbf{F}}_i^\top \bar{\mathbf{Q}}_i + \bar{\mathbf{Q}}_i \bar{\mathbf{F}}_i \leq -\mathbb{I}. \quad (42)$$

321 Let $\bar{V}_i(t) = \bar{\mathbf{x}}_{f_2}^\top \bar{\mathbf{Q}}_i \bar{\mathbf{x}}_{f_2}$, where $V_i(0) = 0$. Differentiating along the system trajectories it follows that

$$322 \begin{aligned} \dot{V}_i &= \bar{\mathbf{x}}_{f_2}^\top (\bar{\mathbf{F}}_i^\top \bar{\mathbf{Q}}_i + \bar{\mathbf{Q}}_i \bar{\mathbf{F}}_i) \bar{\mathbf{x}}_{f_2} + 2\bar{\mathbf{x}}_{f_2}^\top \bar{\mathbf{Q}}_i \bar{\mathbf{G}}_i \tilde{\mathbf{x}} \\ &\leq -\|\bar{\mathbf{x}}_{f_2}\|^2 + 2\|\bar{\mathbf{x}}_{f_2}\| \beta_F \|\tilde{\mathbf{x}}\|_{\mathcal{L}_\infty} \\ &\leq -\|\bar{\mathbf{x}}_{f_2}\|^2 + \beta_F^2 \|\tilde{\mathbf{x}}\|_{\mathcal{L}_\infty}^2 \end{aligned} \quad (43)$$

323 where the last line follows from square completion and $\beta_F = \sqrt{n} \max_{i \in \mathcal{I}} \|\bar{\mathbf{Q}}_i \bar{\mathbf{G}}_i\|$.

324 By integrating it is straightforward to show that the following bound holds for $\bar{\mathbf{x}}_{f_2}$

$$325 \|\bar{\mathbf{x}}_{f_2}\|_{\mathcal{L}_\infty} \leq \kappa_1, \quad (44)$$

326 where $\kappa_1 = \sqrt{n} \max_{i \in \mathcal{I}} \|\bar{\mathbf{Q}}_i \bar{\mathbf{G}}_i\| \delta$ and δ is the upper bound of $\tilde{\mathbf{x}}_i$ defined in Lemma 2.

327 We now define the Lyapunov functions $\bar{W}_i = \bar{\mathbf{e}}^\top \bar{\mathbf{P}}_i \bar{\mathbf{e}}$. Differentiating along the system trajectories

328 it follows that

$$\begin{aligned}
\dot{W}_i &= \bar{\mathbf{e}}^\top (\bar{\mathbf{A}}_i^\top \bar{\mathbf{P}}_i + \bar{\mathbf{P}}_i \bar{\mathbf{A}}_i) \bar{\mathbf{e}} + 2\bar{\mathbf{e}}^\top \bar{\mathbf{P}}_i \bar{\mathbf{H}}_i \bar{\mathbf{x}}_{f_2} + 2\bar{\mathbf{e}}^\top \bar{\mathbf{P}}_i \bar{\mathbf{J}}_i \tilde{\mathbf{x}} \\
&\leq -\|\bar{\mathbf{e}}\|^2 + 2\|\bar{\mathbf{e}}\|\beta_{\bar{\mathbf{e}}}\|\tilde{\mathbf{x}}\|_{\mathcal{L}_\infty} \\
&\leq -\|\bar{\mathbf{e}}\|^2 + \beta_{\bar{\mathbf{e}}}^2\|\tilde{\mathbf{x}}\|_{\mathcal{L}_\infty}^2,
\end{aligned} \tag{45}$$

329 where $\beta_e = \left(\kappa_1 \max_{i \in \mathcal{I}} \|\bar{\mathbf{P}}_i \bar{\mathbf{H}}_i\| + \sqrt{n} \max_{i \in \mathcal{I}} \|\bar{\mathbf{P}}_i \bar{\mathbf{J}}_i\| \right)$.

330 Therefore, the following bound holds

$$331 \quad \|\bar{\mathbf{e}}\|_{\mathcal{L}_\infty} \leq \kappa_2, \tag{46}$$

332 where $\kappa_2 = \left(\kappa_1 \max_{i \in \mathcal{I}} \|\bar{\mathbf{P}}_i \bar{\mathbf{H}}_i\| + \sqrt{n} \max_{i \in \mathcal{I}} \|\bar{\mathbf{P}}_i \bar{\mathbf{J}}_i\| \right) \delta$.

333 Furthermore

$$\begin{aligned}
\|e_u\|_{\mathcal{L}_\infty} &\leq \|\bar{\mathbf{C}}\| \|\bar{\mathbf{e}}\|_{\mathcal{L}_\infty} + \|\bar{\mathbf{L}}_i\| \|\bar{\mathbf{x}}_{f_2}\|_{\mathcal{L}_\infty} + \|\mathbf{D}_f \mathbf{B}_i^\dagger\| \|\tilde{\mathbf{x}}\|_{\mathcal{L}_\infty}, \\
&\leq \kappa_3,
\end{aligned} \tag{47}$$

334 where $\kappa_3 = \|\bar{\mathbf{C}}\| \kappa_2 + \left(\max_{i \in \mathcal{I}} \|\bar{\mathbf{L}}_i\| + \max_{i \in \mathcal{I}} \|\mathbf{D}_f \mathbf{B}_i^\dagger\| \right) \delta$.

335 This completes the proof. □

336 UAV LATERAL-DIRECTIONAL CONTROL IN CASE OF INVERSION OF THE COMMANDS

337 A critical situation in flight control systems is that in case of structural damage of the aircraft,
338 the control direction can be inverted. In fact, if an aircraft suffers damage, a control surface may
339 generate a totally opposite angular acceleration, which means the actuation signs will be changed
340 (Liu et al., 2010; Tan et al., 2017b). The inversion of the sign of the control direction can also
341 result from actuators or software faults. This situation cannot be handled by \mathcal{L}_1 adaptive controller
342 with a single model. Actually, a conservative condition in adaptive control is that the sign of input
343 vector must be known and should not change (Ioannou and Sun, 2012).
344
345

346 Controller Design

347 The lateral-directional equations of motion of a fixed-wing aircraft are described by the set of
 348 states (β, p, r, ϕ) , where β is the sideslip angle, p is the roll rate, r is the yaw rate and ϕ is the roll
 349 angle. The control inputs are the aileron deflection δ_a and the rudder deflection δ_r .

350 The objective is to design a control input $u = [\delta_a, \delta_r]^\top$ to enable tracking of the roll command
 351 ϕ_c and the sideslip angle command β_c .

352 From (Stevens and Lewis, 2003), the linearised model of the lateral-directional dynamics of a
 353 fixed-wing aircraft can be written in matrix form as follows

$$\begin{aligned}
 \underbrace{\begin{bmatrix} \dot{\beta} \\ \dot{p} \\ \dot{r} \\ \dot{\phi} \end{bmatrix}}_{\dot{\mathbf{x}}} &= \underbrace{\begin{bmatrix} \frac{Y_\beta}{V_a} & \frac{Y_p}{V_a} & \frac{Y_r}{V_a} - 1 & \frac{g}{V_a} \\ L_\beta & L_p & L_r & 0 \\ N_\beta & N_p & N_r & 0 \\ 0 & 1 & 0 & 0 \end{bmatrix}}_{\mathbf{A}_p} \underbrace{\begin{bmatrix} \beta \\ p \\ r \\ \phi \end{bmatrix}}_{\mathbf{x}} \\
 &+ \underbrace{\begin{bmatrix} \frac{Y_{\delta_a}}{V_a} & \frac{Y_{\delta_r}}{V_a} \\ L_{\delta_a} & L_{\delta_r} \\ N_{\delta_a} & N_{\delta_r} \\ 0 & 0 \end{bmatrix}}_{\mathbf{B}_p} \underbrace{\begin{bmatrix} \delta_a \\ \delta_r \end{bmatrix}}_{\mathbf{u}},
 \end{aligned} \tag{48}$$

355 where $(Y_\beta, Y_p, Y_r, Y_{\delta_a}, Y_{\delta_r})$, $(L_\beta, L_p, L_r, L_{\delta_a}, L_{\delta_r})$ and $(N_\beta, N_p, N_r, N_{\delta_a}, N_{\delta_r})$ are the lateral-directional
 356 stability derivatives, V_a is the trimmed airspeed and g is the gravity. It should be recalled that the
 357 stability derivatives cannot be measured, and they vary depending on flight conditions.

358 Taking the external disturbances and the model uncertainties into account, the system in (48)
 359 can be extended as follows

$$\dot{\mathbf{x}} = \mathbf{A}_p \mathbf{x} + \mathbf{B}_p \mathbf{u} + \mathbf{f}(t, \mathbf{x}). \tag{49}$$

The system with its nominal desired dynamics can be parameterised to become similar to the class of MIMO systems in (16) defined by

$$\dot{\mathbf{x}} = \mathbf{A}_{m(0)}\mathbf{x} + \mathbf{B}_0(\omega_0\mathbf{u} + \theta_0^\top\mathbf{x} + \eta_{m(0)}) + \eta_{u(0)}(t).$$

A second model for the case of inversion of the sign of the aileron command is given by

$$\dot{\mathbf{x}} = \mathbf{A}_{m(1)}\mathbf{x} + \mathbf{B}_0\beta_1(\omega_1\mathbf{u} + \theta_1^\top\mathbf{x} + \eta_{m(1)}) + \eta_{u(1)}(t),$$

361 where $\beta_1 = \begin{bmatrix} -1 & 0 \\ 0 & 1 \end{bmatrix}$.

A third model for the case of inversion of the sign of the rudder command is given by

$$\dot{\mathbf{x}} = \mathbf{A}_{m(2)}\mathbf{x} + \mathbf{B}_0\beta_2(\omega_2\mathbf{u} + \theta_2^\top\mathbf{x} + \eta_{m(2)}) + \eta_{u(2)}(t),$$

362 where $\beta_2 = \begin{bmatrix} 1 & 0 \\ 0 & -1 \end{bmatrix}$.

A fourth model for the case of inversion of both the signs of the aileron and the rudder commands is given by

$$\dot{\mathbf{x}} = \mathbf{A}_{m(3)}\mathbf{x} + \mathbf{B}_0\beta_3(\omega_3\mathbf{u} + \theta_3^\top\mathbf{x} + \eta_{m(3)}) + \eta_{u(3)}(t),$$

363 where $\beta_3 = \begin{bmatrix} -1 & 0 \\ 0 & -1 \end{bmatrix}$.

364 The input matrix B_0 was taken to be the same for both models.

365 **Simulation Results**

366 In order to show the efficiency of the multiple model controller, simulations were first made
367 using only the nominal controller, i.e., the \mathcal{L}_1 adaptive controller with one model. Two situations

368 were considered in this case:

- 369 1. Control inputs loss of effectiveness of 50% without the inversion of the commands;
- 370 2. Control inputs loss of effectiveness of 50% with the inversion of the sign of the aileron
- 371 command.

372 Furthermore, the following uncertainties were added to the plant at simulation time $t = 7$ s:

- 373 • Linear-in-state unknown parameters;
- 374 • Matched disturbance $d_m = \sin(2\pi t)$ deg.

375 Simulation results for the nominal \mathcal{L}_1 adaptive controller, without inversion of actuation signs,
376 are shown in Figure 3. As expected, the system has good performance in the presence of uncer-
377 tainties. The aileron command δ_a and the rudder command δ_r are within acceptable limits.

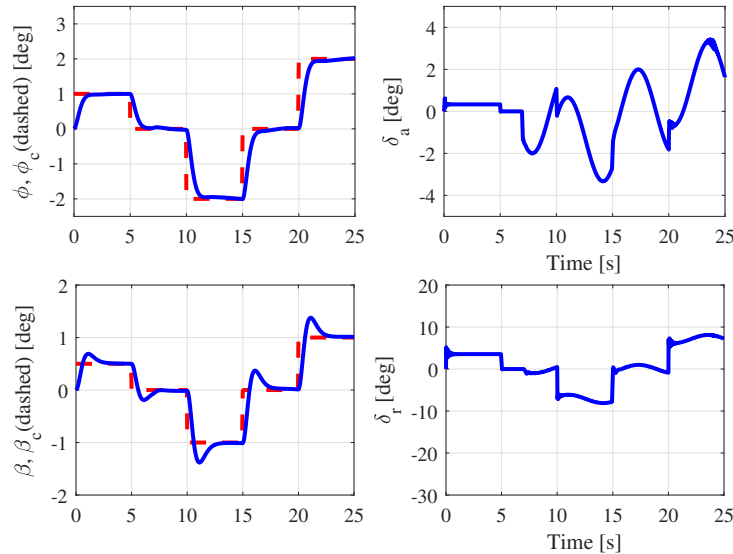


Fig. 3. Closed-loop tracking performance of the nominal controller without inversion of the sign of the commands.

378 In the second scenario of loss of effectiveness of 50% with the inversion of the sign of the
379 aileron command, the system with only the nominal controller has become unstable as it can be
380 observed in Figure 4. This is a direct consequence of the fact the adaptation laws (7)-(11) cannot
381 match the correct control direction when it is inverted.

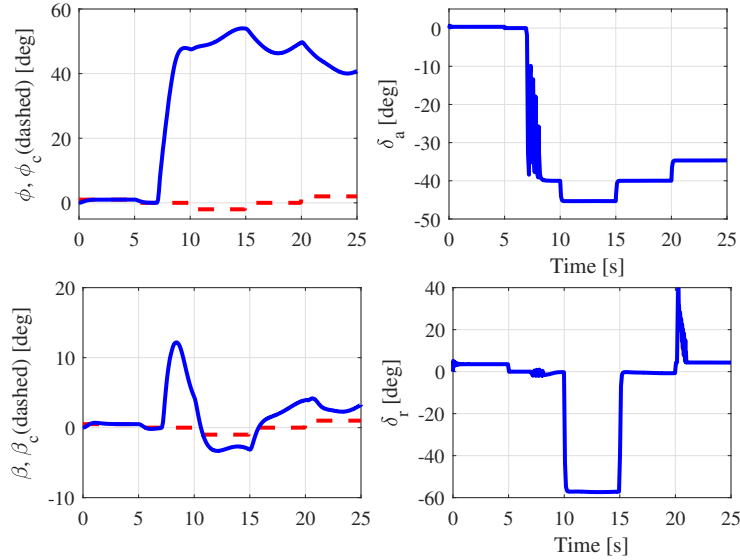


Fig. 4. Closed-loop tracking performance of the nominal controller with inversion of the sign of the aileron.

382 Next, the multiple model controller was applied. The tuning parameters and the desired
 383 dynamics of the suboptimal controller were the same as the nominal controller. Three situations
 384 were considered in simulations:

- 385 1. Control inputs loss of effectiveness of 50% with the inversion of the sign of the aileron
 386 command;
- 387 2. Control inputs loss of effectiveness of 50% with the inversion of the sign of the rudder
 388 command;
- 389 3. Control input loss of effectiveness of 50% with the of both the signs of the aileron and the
 390 rudder commands.

391 Moreover, the same uncertainties as in previous simulations were added to the plant. The failures
 392 were introduced at simulation time $t = 7$ s.

393 The simulation results in the case of inversion of the sign of aileron command, the rudder
 394 command, and both the ailerons and the rudder commands, are shown in Figure 5, Figure 6 and
 395 Figure 7, respectively. In each situation, the system has stayed stable and has shown a good tracking
 396 performance. The aileron command δ_a and the rudder command δ_r were within acceptable limits.

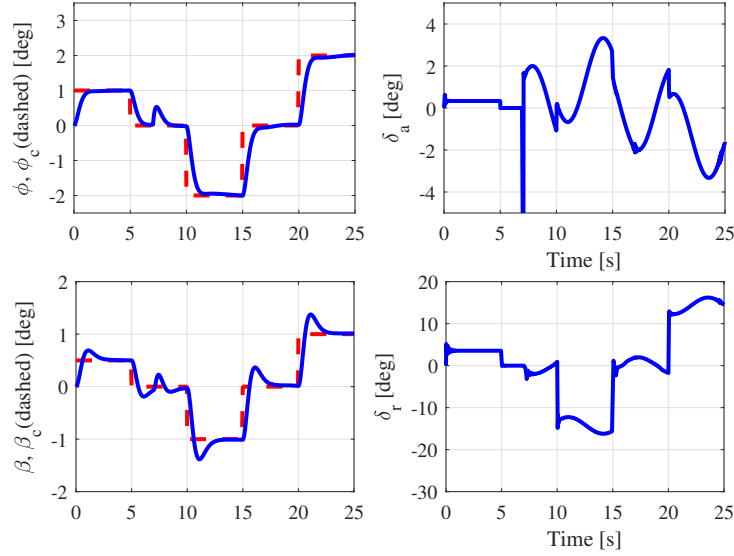


Fig. 5. Closed-loop tracking performance of the multiple model controller with inversion of the sign of the aileron.

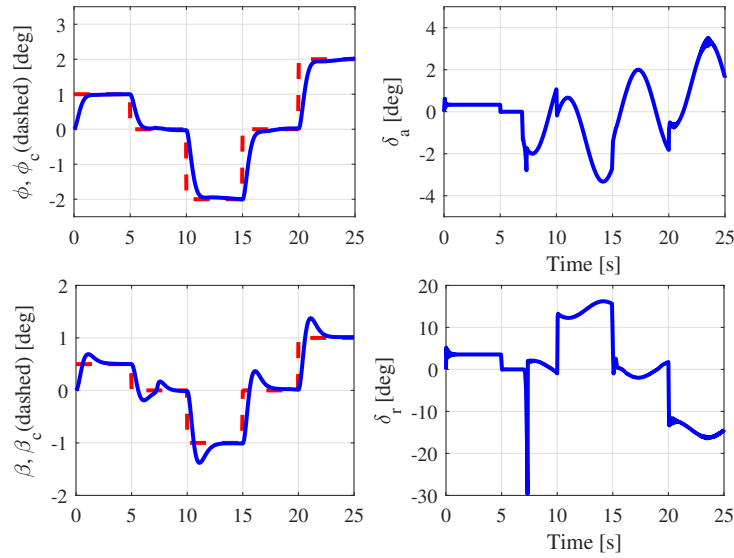


Fig. 6. Closed-loop tracking performance of the multiple model controller with inversion of the sign of the rudder.

397 Furthermore, as it is shown on Figure 8, the matching model to each failure case corresponds
 398 to the minimum cost function defined in (23).

399 These simulations conclude that the application of the multiple model \mathcal{L}_1 adaptive controller is
 400 justified in case of structural damages or faults that lead to inversion of the sign of the control input
 401 of flight systems.

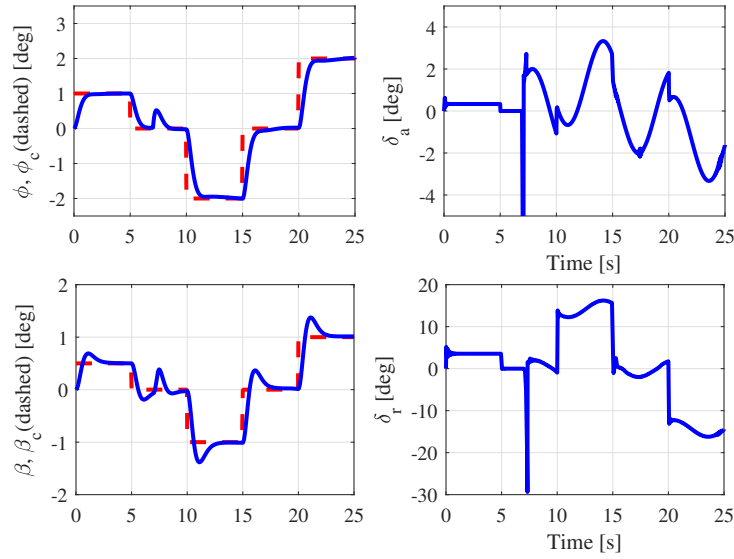
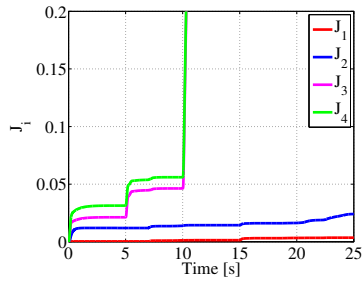
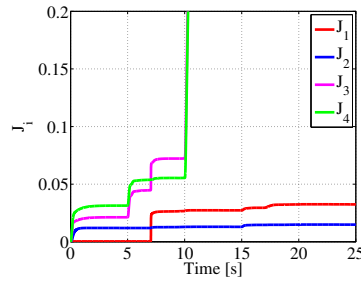


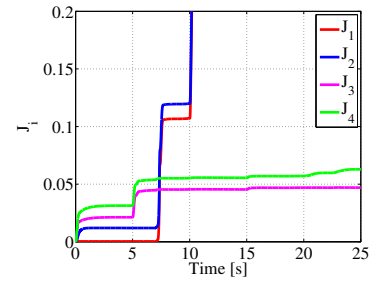
Fig. 7. Closed-loop tracking performance of the multiple model controller with inversion of the sign of both the aileron and the rudder.



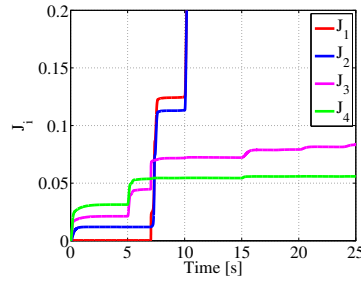
(a) 1st failure case.



(b) 2nd failure case.



(c) 3rd failure case.



(d) 4th failure case.

Fig. 8. Cost Functions

402 **SUMMARY**

403 In this paper, an approach for \mathcal{L}_1 adaptive fault-tolerant control MIMO systems is proposed.
 404 The aim is the fault-tolerant control of small fixed-wing UAVs in the presence of critical failures.

405 The design is based on a nominal model for a fault-free plant and a set of suboptimal models for the
406 plant under failures. The switching between the models is based on a simple quadratic criterion.

407 The main advantage of this approach is that it allows a larger class of uncertainties and faults to
408 be considered and can achieve better accommodation and preserve system integrity. Simulations
409 have shown that the multiple model \mathcal{L}_1 adaptive has stabilised the system in case of inversion of
410 the control input, while the controller with a single model has failed.

411 **PRACTICAL APPLICATIONS**

412 Small drones or Unmanned Aerial Vehicles (UAVs) that is, with wingspans less than 2 metres
413 and payload smaller than 2 kg, are generally built based on commercial Radio Controlled (RC)
414 airplane. Small UAVs are gaining growing interest because of their low cost, high manoeuvrability
415 and simple maintenance. Autonomy, although relative because they are still operated under human
416 supervision, is the main feature of small UAVs compared to RC airplane. Autonomy has been made
417 possible through the development of advanced autopilot (flight control) systems. They are used for a
418 wide range of military and civilian tasks, such as: inspection, detection, transportation, monitoring,
419 search and rescue, photography, imaging, mapping, intelligence, surveillance, reconnaissance,
420 agriculture, entertainment etc. However, small UAVs are generally built with low-cost components
421 and materials, which increases the probability of occurrence of faults and failures. The proposed
422 flight control solution permits to maintain the UAVs in flight in the presence of hard failure, while
423 other approaches fail. Therefore, the mission can be safely terminated, either automatically, or
424 manually. Alternatively, it it can also be decided to complete the operation in degraded (limited)
425 mode. Therefore, this solution is recommended for the operation of drones, especially in urban
426 environments that needs a high degree of safety and reliability.

427 **DATA AVAILABILITY STATEMENT**

428 The data that support the findings of this study are available from the author upon reasonable
429 request.

ACKNOWLEDGEMENTS

I would like to express my gratitude to my PhD supervisor Pr. Walter Fichter, University of Stuttgart, for his guidance and detailed advice through the elaboration of this research. I would also like to express my appreciation to my thesis referee Professor Florian Holzapfel for his insights and comments.

REFERENCES

- Abbaspour, A., Mokhtari, S., Sargolzaei, A., and Yen, K. K. (2020). “A survey on active fault-tolerant control systems.” *Electronics*, 9(9), 1513.
- Ackerman, K. A., Xargay, E., Choe, R., Hovakimyan, N., Cotting, M. C., Jeffrey, R. B., Blackstun, M. P., Fulkerson, T. P., Lau, T. R., and Stephens, S. S. (2017). “Evaluation of an \mathcal{L}_1 adaptive flight control law on calspan’s variable-stability learjet.” *Journal of Guidance, Control, and Dynamics*, 40(4), 1051–1060.
- Ahmadi, K., Asadi, D., and Pazooki, F. (2019). “Nonlinear \mathcal{L}_1 adaptive control of an airplane with structural damage.” *Proceedings of the Institution of Mechanical Engineers, Part G: Journal of Aerospace Engineering*, 233(1), 341–353.
- Amin, A. A. and Hasan, K. M. (2019). “A review of fault tolerant control systems: advancements and applications.” *Measurement*, 143, 58–68.
- Austin, R. (2011). *Unmanned aircraft systems: UAVs design, development and deployment*, Vol. 54. John Wiley & Sons.
- Benosman, M. (2011). “Passive fault tolerant control.” *Robust Control Theory Appl.*
- Blanke, M., Kinnaert, M., Lunze, J., Staroswiecki, M., and Schröder, J. (2006). *Diagnosis and fault-tolerant control*, Vol. 2. Springer.
- Bodson, M. (2003). “Reconfigurable nonlinear autopilot.” *Journal of Guidance, Control, and Dynamics*, 26(5), 719–727.

454 Cao, C. and Hovakimyan, N. (2008). “Design and analysis of a novel \mathcal{L}_1 adaptive control architec-
455 ture with guaranteed transient performance.” *IEEE Transactions on Automatic Control*, 53(2),
456 586–591.

457 Cao, C. and Hovakimyan, N. (2009). “L1 adaptive output-feedback controller for non-strictly-
458 positive-real reference systems: missile longitudinal autopilot design.” *Journal of guidance,
459 control, and dynamics*, 32(3), 717–726.

460 Dobrokhodov, V., Xargay, E., Hovakimyan, N., Kaminer, I., Cao, C., and Gregory, I. M. (2013).
461 “Multicriteria analysis of an \mathcal{L}_1 adaptive flight control system.” *Proceedings of the Institution of
462 Mechanical Engineers, Part I: Journal of Systems and Control Engineering*, 227(4), 413–427.

463 Ducard, G. J. (2009). *Fault-tolerant flight control and guidance systems: Practical methods for
464 small unmanned aerial vehicles*. Springer.

465 Edwards, C., Spurgeon, S. K., and Akoachere, A. (2000). “A sliding mode static output feedback
466 controller based on linear matrix inequalities applied to an aircraft system.” *Journal of Dynamic
467 Systems, Measurement, and Control*, 122(4), 656–663.

468 Hovakimyan, N. and Cao, C. (2010). *\mathcal{L}_1 adaptive control theory: Guaranteed robustness with fast
469 adaptation*, Vol. 21. Siam.

470 Hwang, I., Kim, S., Kim, Y., and Seah, C. E. (2009). “A survey of fault detection, isolation, and
471 reconfiguration methods.” *IEEE transactions on control systems technology*, 18(3), 636–653.

472 Ioannou, P. A. and Sun, J. (2012). *Robust adaptive control*. Courier Dover Publications.

473 Jiang, J. and Yu, X. (2012). “Fault-tolerant control systems: A comparative study between active
474 and passive approaches.” *Annual Reviews in control*, 36(1), 60–72.

475 Jiang, J. and Zhang, Y. (2006). “Accepting performance degradation in fault-tolerant control system
476 design.” *Control Systems Technology, IEEE Transactions on*, 14(2), 284–292.

477 Lavretsky, E. and Wise, K. A. (2013). “Robust adaptive control.” *Robust and Adaptive Control*,
478 Springer, 317–353.

479 Liberzon, D. (2003). *Switching in systems and control*. Springer Science & Business Media.

480 Liu, Y., Tao, G., and Joshi, S. M. (2010). “Modeling and model reference adaptive control of aircraft
481 with asymmetric damage.” *Journal of Guidance, Control, and Dynamics*, 33(5), 1500–1517.

482 Ma, Y., Jiang, B., Tao, G., and Badihi, H. (2020). “Minimum-eigenvalue-based fault-tolerant
483 adaptive dynamic control for spacecraft.” *Journal of Guidance, Control, and Dynamics*, 43(9),
484 1764–1771.

485 Mühlegg, M., Niermeyer, P., Falconi, G. P., and Holzapfel, F. (2015). “ \mathcal{L}_1 fault tolerant adaptive
486 control of a hexacopter with control degradation.” *2015 IEEE Conference on Control Applications*
487 *(CCA)*, IEEE, 750–755.

488 Narendra, K. S. and Balakrishnan, J. (1997). “Adaptive control using multiple models.” *IEEE*
489 *transactions on automatic control*, 42(2), 171–187.

490 Nian, X., Chen, W., Chu, X., and Xu, Z. (2020). “Robust adaptive fault estimation and fault tolerant
491 control for quadrotor attitude systems.” *International Journal of Control*, 93(3), 725–737.

492 Patel, V. V., Cao, C., Hovakimyan, N., Wise, K. A., and Lavretsky, E. (2009). “ \mathcal{L}_1 adaptive controller
493 for tailless unstable aircraft in the presence of unknown actuator failures.” *International Journal*
494 *of Control*, 82(4), 705–720.

495 Patton, R. J. (1997). “Fault-tolerant control: the 1997 situation.” *IFAC Proceedings Volumes*,
496 30(18), 1029–1051.

497 Rotondo, D. (2017). *Advances in gain-scheduling and fault tolerant control techniques*. Springer.

498 Snyder, S. (2019). “L1 adaptive control within learn-to-fly.” Ph.D. thesis, University of Illinois at
499 Urbana-Champaign, University of Illinois at Urbana-Champaign.

500 Sørensen, M. E. N. and Breivik, M. (2015). “Unmanned aerial vehicle fault-tolerant control
501 by combined \mathcal{L}_1 adaptive backstepping and fault-dependent control allocation.” *2015 IEEE
502 Conference on Control Applications (CCA)*, IEEE, 1880–1886.

503 Souanef, T. (2019). *Adaptive Guidance and Control of Small Unmanned Aerial Vehicles*. Shaker
504 Verlag, Germany.

505 Souanef, T., Boubakir, A., and Fichter, W. (2015). “ \mathcal{L}_1 adaptive control of systems with disturbances
506 of unknown bounds.” *Advances in Aerospace Guidance, Navigation and Control*, Springer, 151–
507 165.

508 Souanef, T. and Fichter, W. (2015). “Fault tolerant \mathcal{L}_1 adaptive control based on degraded models.”
509 *Advances in Aerospace Guidance, Navigation and Control*, Springer, 135–149.

510 Stevens, B. L. and Lewis, F. L. (2003). *Aircraft Control and Simulation*. Wiley, New York.

511 Tan, C., Tao, G., Qi, R., and Yang, H. (2017a). “A direct MRAC based multivariable multiple-model
512 switching control scheme.” *Automatica*, 84, 190–198.

513 Tan, C., Tao, G., Yang, H., and Xu, F. (2017b). “A multiple-model adaptive control scheme
514 for multivariable systems with uncertain actuation signs.” *2017 American Control Conference
515 (ACC)*, IEEE, 1121–1126.

516 Tao, G. (2004). *Adaptive control of systems with actuator failures*. Springer.

517 Tian, S., Wang, J., Lin, D., and Pei, P. (2020). “ \mathcal{L}_1 adaptive control design of a helicopter in vertical
518 flight.” *Proceedings of the Institution of Mechanical Engineers, Part G: Journal of Aerospace
519 Engineering*, 234(14), 2089–2099.

520 Valavanis, K. P. and Vachtsevanos, G. J. (2015). *Handbook of Unmanned Aerial Vehicles*. Springer.

521 Wang, J. (2010). “Robust and nonlinear control literature survey (no. 19).” *International Journal
522 of Robust and Nonlinear Control*, 20(12), 1427–1430.

- 523 Xue, Y., Zhen, Z., Yang, L., and Wen, L. (2020). “Adaptive fault-tolerant control for carrier-based
524 uav with actuator failures.” *Aerospace Science and Technology*, 107, 106227.
- 525 Yang, F., Zhang, H., Jiang, B., and Liu, X. (2014). “Adaptive reconfigurable control of systems with
526 time-varying delay against unknown actuator faults.” *International Journal of Adaptive Control
527 and Signal Processing*, 28(11), 1206–1226.
- 528 Yang, G.-H., Wang, J. L., and Soh, Y. C. (2001). “Reliable controller design for linear systems.”
529 *Automatica*, 37(5), 717–725.
- 530 Zang, Z. and Bitmead, R. R. (1990). “Transient bounds for adaptive control systems.” *29th IEEE
531 Conference on Decision and Control*, IEEE, 2724–2729.
- 532 Zhang, Y. and Jiang, J. (2003). “Fault tolerant control system design with explicit consideration
533 of performance degradation.” *IEEE Transactions on Aerospace and Electronic Systems*, 39(3),
534 838–848.
- 535 Zhang, Y. and Jiang, J. (2008). “Bibliographical review on reconfigurable fault-tolerant control
536 systems.” *Annual Reviews in Control*, 32(2), 229–252.
- 537 Zhou, Y., Liu, H., Guo, H., and Duan, X. (2019). “ \mathcal{L}_1 adaptive dynamic inversion attitude control
538 for unmanned aerial vehicle with actuator failures.” *Proceedings of the Institution of Mechanical
539 Engineers, Part G: Journal of Aerospace Engineering*, 233(11), 4129–4140.

540
541
542
543
544
545
546
547
548
549
550
551
552
553

List of Figures

1	Block diagram of the \mathcal{L}_1 adaptive controller.	6
2	Block diagram of the multiple model \mathcal{L}_1 adaptive controller.	10
3	Closed-loop tracking performance of the nominal controller without inversion of the sign of the commands.	23
4	Closed-loop tracking performance of the nominal controller with inversion of the sign of the aileron.	24
5	Closed-loop tracking performance of the multiple model controller with inversion of the sign of the aileron.	25
6	Closed-loop tracking performance of the multiple model controller with inversion of the sign of the rudder.	25
7	Closed-loop tracking performance of the multiple model controller with inversion of the sign of both the aileron and the rudder.	26
8	Cost Functions	26

2023-11-09

Multiple model L1 adaptive fault-tolerant control of small unmanned aerial vehicles

Souanef, Toufik

American Society of Civil Engineers

Souanef T. (2024) Multiple model L1 adaptive fault-tolerant control of small unmanned aerial vehicles. *Journal of Aerospace Engineering*, Volume 37, Issue 1, January 2024

<https://doi.org/10.1061/JAEEZ.ASENG-4427>

Downloaded from Cranfield Library Services E-Repository